Journal of Energy Storage 133 (2025) 118023

Contents lists available at ScienceDirect

Journal of Energy Storage

journal homepage: www.elsevier.com/locate/est

Research Papers

Development of ternary blended cements (LC^3) to be applied as thermal energy storage material in concentrated solar power plants

L. Betancor-Cazorla, Carlos A. Vielma, J. Mañosa, S. Dosta, J.M. Chimenos, C. Barreneche *

Departament de Ciència de Materials i Química Física, Universitat de Barcelona, C/Martí i Franqués 1, 08028 Barcelona, Spain

ARTICLE INFO

Keywords:
Thermal energy storage (TES)
Concentrated solar power (CSP) plants
Metakaolin
Mechanical activation
Limestone calcined clay cement (LC^3)
Life cycle assessment (LCA)

ABSTRACT

Currently, there is great awareness of the increase in energy consumption, dependence on fossil fuels, and greenhouse gas emissions, particularly CO_2. One of the largest sources of carbon dioxide emissions is the cement and concrete industry, which has been growing in recent years. Therefore, it is necessary to implement measures to limit the global pollution caused by this sector. Furthermore, with the development of renewable energies, there is a growing need to develop batteries and materials that allow to store this energy for later use. Therefore, the main objective of this study is the development of ternary blended cements (LC^3), in which clinker is partially replaced by thermally and mechanically activated kaolinitic clay, to be implemented as a thermal storage material in CSP plants. The development of the alternative cements was carried out in the laboratory and a full characterization was performed to evaluate their physical, mechanical, and thermal properties. In addition, a comparison of these properties with Portland cements was performed, to evaluate whether the characteristics presented met the required needs. Therefore, LC^3 cements have affordable energy storage capacity to be implemented as TES media. In addition, LC^3 cements have the same storage capacity as OPC, and it is maintained after aging test. Finally, an LCA was performed to quantify and evaluate the reductions provided by LC^3 in terms sustainability reduction impact in the environment to be using this alternative cement in comparison with the common one. The results showed that both the mechanical and thermal properties of the cements are in line with the expected values and allow their use as TES materials regarding the energy storage capacity, energy density and energy performance by achieving and environmental impact reduction up to 22,6 %. Therefore, this study confirms that LC^3 cement is more sustainable cements that significantly reduce CO_2 eq. emissions (up to 24 % reduction).

1. Introduction

Currently, there is significant concern about the increase in energy consumption, dependence on fossil fuels, and greenhouse gas (GHG) emissions, especially carbon dioxide (CO_2) [1]. As a result, countries are increasingly aware of the need to reduce this effect and are developing government policies accordingly. Likewise, different international treaties have been appearing, which aim to set up common environmental objectives for the different countries, such as the Paris Agreement [2] and the European Green Pact of the year 2019. This Pact aims to reduce the 55 % greenhouse gas emissions by 2030 and achieve climate neutrality by 2050 [3]. In addition, the increased implementation of renewable energies brought with it the need to develop storage materials to store this energy. An example is the use of CSP plants with a thermal energy storage (TES) system. In this way, the solar energy is transformed into heat that is stored in a material (e.g. molten salts or solid particles) [4]. This type of power plant has several advantages, such as the simplicity of energy handling (transport, and storage) and the reduction of energy dependence, especially in less developed countries [5]. One of the TES systems that has been studied in recent years is the concrete unit used as TES media. Concrete is an inexpensive material that is easy to obtain and design. It can withstand high temperatures and is highly resistant to corrosion. In addition, cement does not require being inside a container like other TES systems [5,6].

The first concrete storage prototype was tested at the Plataforma Solar de Almeria (Spain) during 2003–2004, a project approved by the German government and carried out by the German Aerospace Center [7]. Subsequently, another concrete storage project was carried out by them (DLR) in Stuttgart (Germany), focusing on the cost reduction [8]. In recent years, the Plataforma Solar de Almería has been working on a project called *E*-CRETE PROJECT (Energy storage solutions based on

---

* Corresponding author.
E-mail address: c.barreneche@ub.edu (C. Barreneche).

https://doi.org/10.1016/j.est.2025.118023
Received 17 December 2024; Received in revised form 22 April 2025; Accepted 6 August 2025

Glossary

C_p	Heat capacity
CSP	Concentrated Solar Power
GHG	Greenhouse gas
k	Thermal conductivity
LC^3	Limestone Calcined Clay Cement
LCA	Life Cycle Assessment
LCI	Life Cycle Inventory
LCIA	Life Cycle Inventory Analysis
MA	Mechanically Activated kaolin
MK	Metakaolin (Thermally Activated kaolin)
OPC	Ordinary Portland Cement
PC	Portland Cement
SCMs	Supplementary Cementitious Materials
SP	Superplasticiser
TES	Thermal Energy Storage
w/b	water/binder
YSZ	Yttria-stabilized zirconium oxide
ρ_{bulk}	Bulk density
ρ_{real}	Real density
ρ_e	Volumetric heat capacity
σ_c	Compressive strength
φ	Porosity

CONCRETE) [9]. This research is based on using concrete that increases thermal performance and durability as a TES unit. The idea is to convert the laboratory results [10–12] to a more practical scale, integrating them into applications for power generation, industrial energy recovery and thermal plants. In addition, there are the Zhangbei and Zhangjiakou CSP plants in China (50 MW) where TES concrete units were introduced to provide 14 h storage [13]. Moreover, in 2018 CADE started the EDITOR CSP project with solid-TES system [14]. In this project, they have been supplying process steam continuously to the KEAN soft drinks factory in Limassol (Cyprus).

However, one of the main disadvantages of the use of concrete as a material for TES applications is that it is one of the world's largest sources of CO_2 emissions [15]. In 2020, 14 billion cubic meters (bcm) of concrete and 4.2 billion tons of cement were produced, which could lead to a total of 3.8 Gt of CO_2 in 2050 if no measures are implemented [16]. These associated emissions come mainly from the CO_2 emissions generated during the calcination of limestone ($CaCO_3$) to produce clinker (mainly composed of CaO), the base material in Portland cement (PC). In addition, there are emissions associated with the burning of fossil fuels necessary to achieve the high temperature required for the kilns (1400–1500 °C). Therefore, there are direct scope 1 emissions classified under the Greenhouse Gas Protocol [17]. To address this main issue, there are several solutions to reduce the environmental impact of cement and, consequently, of concrete. One of the options lies in the partial substitution of clinker by other more sustainable materials (supplementary cementitious materials, SCMs), such as clay. Thereby, in this work, kaolin will be used to substitute clinker, mainly due to its kaolinite content which has been studied for its reactivity and pozzolanic behavior to replace cement [18,19]. However, these properties depend on the composition of the mineral, the activation conditions, and the grain size of the final product [20,21]. If the activation is performed thermally, calcined kaolinite forms metakaolinite, changing from a crystalline material to an amorphous structure with good properties as SCM [20]. With the combination of calcined clay and limestone as SCMs, a ternary blended cement known as limestone calcined clay cement (LC^3) is obtained, with comparable or superior performance to PC.

The temperature at which the highest reactivity occurs is within the range of 600 °C to 850 °C for 1 h to 12 h [18,19]. Similar transformations that activated kaolin undergoes thermally, can also be undergone mechanically. The mechanical kaolin activation is performed using grinding equipment such as ball or roller mills. In addition, grinding must achieve an extremely high fineness of the material to increase its reactivity and facilitate its use as a clinker replacement [22].

This work aims to develop and characterize ternary blended cements to reduce the environmental impact of concrete TES systems in CSP plants. To fulfil this objective, a study of the physicochemical, mechanical, and thermal properties of blended cements produced with thermally and mechanically activated kaolin and limestone was carried out. In addition, a Life Cycle Assessment (LCA) was also performed to evaluate the environmental impact and sustainability of these materials.

2. Materials and methods

2.1. Materials

The clay used in this project was high-purity commercial kaolin (82 wt% of kaolinite) provided by Minerals i Derivats, S.A. (Spain), and had to be activated. This activation was carried out thermally and mechanically to compare the cements obtained with both processes.

The clinker used was provided by Cementos Molins, S.A. It was crushed into small pieces in a jaw crusher and ground in a ring mill for 6 min at 700 rpm. Samples of 100–120 g were used to ensure a good grind. Once ground, the clinker was sieved on an 80 μm nominal aperture sieve.

Portland cement was supplied by Cementos Molins, S.A. Two types were used: DRAGON cement, with limestone type CEM II/B-L of resistance category 32.5 N and DRAGON SR cement of medium-high final resistance, type CEM I. Type D consists of 70 % clinker and 30 % limestone and type SR consists of 94 % clinker and 6 % limestone.

Commercial gypsum and limestone were supplied by LABKEM (Labbox, Spain), with purities of >99 % and > 98.5 %, respectively.

2.2. Kaolin activation methodology

Thermal activation was carried out in a muffle furnace. Samples of 80 g of kaolin were introduced and calcined at 800 °C for 1 h to obtain metakaolin (MK). For this purpose, a heating ramp was programmed, from room temperature to 300 °C with a heating rate of 2.5 °C/min and from 300 °C to 800 °C at 5 °C/min. After one hour at this temperature in the furnace, the samples were cooled down to room temperature. In this way, the samples spent 4 and a half hours in the muffle furnace. Mechanical activation was carried out to obtain mechanically activated (MA) kaolin in a PM 400 planetary ball mill (RETSCH) for 1 h at 300 rpm. Yttria-stabilized zirconium oxide (YSZ) 500 ml jars were used and 160 YSZ balls per jar were introduced. The mass ratio of kaolin/balls was 1/20, based on the preliminary test to fill 20 % of the volume of the jars.

2.3. Cement preparation methodology

For the preparation of PC and LC^3, samples of 100 g of cement were made with the following formulation (Table 1). Four types of cement were prepared: a) LC^3 with thermally activated kaolin (MK), b) LC^3 with mechanically activated kaolin (MA), c) Portland D, and d) Portland SR. In addition, to use the same amount of water for all four cements, a polycarboxylate ether-based superplasticiser (SP) provided by CHRYSO was added to the LC^3s since clay absorbs a lot of water. In this way, the same water/binder ratio (w/b) was used, where the binder is the total mass of solid materials. Similarly, the amount of PS is also calculated from the total mass of solid materials.

The mixing procedure was the same for LC^3s as for PCs (Fig. 1). First, the solids were weighed and mixed, and the water was separated for

Table 1
Mix designs of the different cements considered in this study.

Cement type		Solid Materials (wt%)				Liquid Materials	
		Clinker	Kaolin	$CaCO_3$	Gypsum	w/b	SP (%)
LC^3	Thermal activation (MK)	50	30	15	5	0.40	0.90
	Mechanical activation (MA)	50	30	15	5	0.40	0.55
PC	Portland D	70	–	30	–	0.40	–
	Portland SR	94	–	6	–	0.40	–

each sample. For mechanically activated kaolin, 70 % of the corresponding water was weighed in one beaker and 30 % in another beaker with 0.55 % SP. For metakaolin, 80 % of the corresponding water was weighed in one beaker and 20 % with 0.90 % SP in another beaker. Subsequently, the solids were mixed for 2 min until a homogeneous mixture was obtained. Water was added and mixed at low speed to impregnate the entire solid for 2 min and the rest of the water with the SP was added and mixed at high speed for 2.5 min. However, for D and SR Portland cement, the addition of SP was not necessary, so water was added at once. In this case, 100 g of each type of cement (Portland D and SR) were weighed, having the composition specified in Table 1. Once finished, 2.5 cm molds were filled, and air was removed to avoid pore formation. For curing, the samples were sealed in a plastic bag for 24 h. Finally, the demolded cements were left to cure in the climatic chamber at 20 °C and 95 % relative humidity for 28 days. A total of six samples of each type of cement were prepared.

2.3.1. *Aging*

The cement samples were aged in a muffle furnace to study thermal fatigue behavior. For this purpose, the cement samples were heated in a furnace at 350 °C for 500 h. After this time, DSC and compression tests were performed again after the aging test.

2.4. *Characterization*

The characterization techniques used in this study are divided according to determine the physicochemical, mechanical, and thermal properties of the materials. Notice that the samples were aged in an oven at 350 °C to compare their properties before and after.

2.4.1. *Mechanical and physicochemical properties*

2.4.1.1. Compressive strength test. The **compressive strength (σ_c)** was performed on both LC^3 and PC samples. It was carried out in an Incotecnic universal testing machine, according to EN 196–1 standard, in which compressive stresses were applied until they broke.

2.4.1.2. Densities and porosity. The **bulk density (ρ_{bulk})** was calculated for each sample using the weight and the volume. Five weighings were carried out on each sample (six samples for each type of cement), and all sides of each sample were measured three times with a calliper. The AccuPyc 1330 helium Pycnometer was used to measure the **real density (ρ_{real})**. This, from a fixed volume of helium, whose density is known, is able to determine the density of the sample from Archimedes' principle. From the displaced volume and the weighed mass, the pycnometer determined the density for LC^3 and both Portland cements. To ensure that all the pores were accessible to the intrusion of the helium, the samples to be measured were crushed into small pieces, and the vessel of known volume was filled with a known amount of sample for each type of cement.

The **porosity (ϕ)** of the material was given by the ratio between the volume occupied by the pores and the total volume of the sample. From the data obtained in the previous tests, the porosity was calculated.

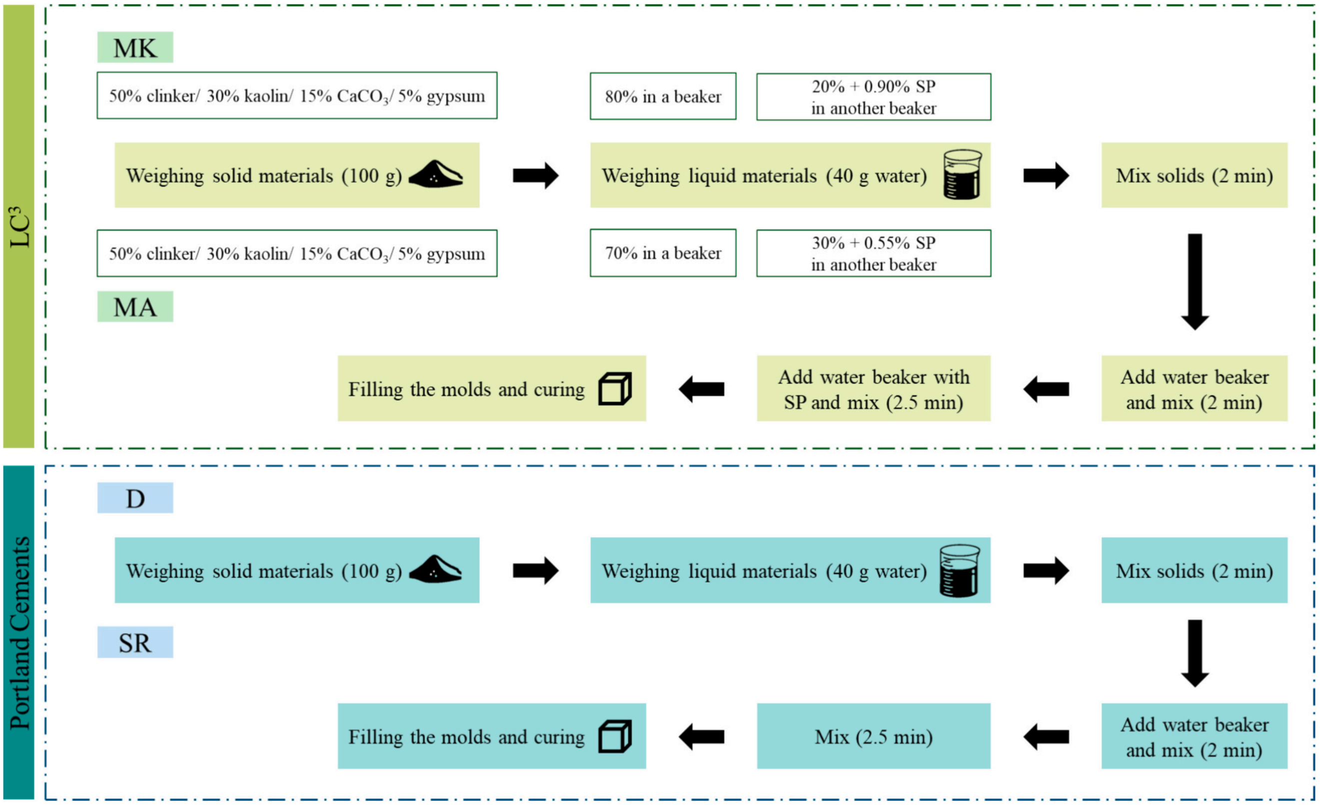

Fig. 1. Schematic diagram of the synthesis process.

2.4.1.3. X-ray diffraction (XRD). The test was performed with PANalytical X'Pert PRO MPD alpha1 powder diffractometer in Bragg-Brentano θ/2 θ geometry of 240 mm of radius. 8 solid powder samples were mounted backloaded in the cylindrical cavity, of 16 mm in diameter and 2.5 mm in thickness of standard (PW1811/16) sample holders. Four samples, one of each cement before aging, and four samples, one of each cement after aging were measured. The measurements were obtained in continuous scan mode and the 2θ range from 4° to 100° with a step size of 0.026° 2θ and a measuring time of 200 s per step.

2.4.2. Thermal properties

2.4.2.1. Differential scanning calorimetry (DSC). To carry out the analysis, a known mass of each type of cement was placed in a 40 μl aluminum crucible. The behavior of the materials was studied at 300–350-400 °C in N_2 atmosphere (50 ml·min^{-1}). For the calculation of **heat capacity, C_p**, sapphire was used as a standard following the area method [23]. The C_p (J·g^{-1}·°C^{-1}) was obtained with Eq. (1), where A is the integrated peak area for the material curve, and A_s is the integrated peak area for the sapphire curve in J·kg^{-1} and $C_{p,s}$ is the heat capacity of the sapphire in J·g^{-1}·°C^{-1}. Also, for a better understanding of the thermal storage capacity of types of cement, the **volumetric heat capacity (ρ_e)** in MJ·m^{-3}·°C^{-1} was determined following **Eq. (2)**, where the density (ρ_{bulk}) is that obtained previously in kg·m^{-3} and C_p is the heat capacity of the cements in J·kg^{-1}·°C^{-1}.

$$C_p = \frac{C_{p,s} \bullet A}{A_s} \tag{1}$$

$$\rho_e = \rho_{bulk} \bullet C_p \tag{2}$$

2.4.2.2. Thermal conductivity. The **thermal conductivity (k)** of the cement was measured following the Hot Wite method using a KD2 Pro Thermal Properties Analyzer manufactured by Decagon Devices Inc. The RK-1 sensor was used, as it is suitable for solid rock and cured concrete. Five measurements were made for 10 min in High Power Mode for each sample, with a waiting time of 20 min between measurements at room temperature.

3. Results and discussion

3.1. Physicochemical and mechanical properties

Table 2 shows the results obtained for each property studied before and after thermal aging. Regarding compressive strength, the results of LC^{3}s were in concordance with those reported in the literature [19,22]. Both presented values around 40 MPa, which implies that the mechanical and thermal amorphization of the kaolin (using 30 % of it in the mixture) was enough to achieve adequate strength values. In addition, in some MA samples, the strength was higher than that of MK due to the grinding degree of the clay. This allowed better packing and, therefore, a quick and efficient reaction [22,24].

These results are perfectly comparable to the results provided by the Portland cement manufacturer [25]. However, these values have been measured at room temperature and, in their use as a TES system, these materials must operate in conditions of 200–400 °C. This requirement is fundamental since heating the concrete produces a series of reactions and transformations that affect the compressive strength, which typically decreases by 20 % when exceeding 400 °C [26]. For this reason, after thermal aging at 350 °C, the compression test was repeated. The results showed a significant reduction of almost 50 % for LC^{3}s and 70 % for PCs. Nevertheless, the ternary blended cements are still within the range indicated in the literature [6], and the results were comparable to those of other studies [26], ensuring structural integrity and prolonging the service life of the system. In addition, as the cements showed clear signs of fracture, this may have influenced the values obtained. Thereby, the mechanical test confirms that the usage of this more sustainable cements as TES materials to store energy in CSP plants is as viable as the usage of OPC ones.

On the other hand, apparent density results showed similar densities between Portland cements and LC^{3}s, being slightly lower for LC^{3}s, and conformed to the manufacturer's specifications and literature, respectively [25,27]. This was due to the clinker content being 50 %, indicating the partial replacement of clinker with thermally and mechanically activated kaolin did not affect the density of the material, which continued to comply with the values specified in the Código Técnico de la Edificación in Spain [28]. Portland SR, which had a high clinker content of 94 %, showed a higher density. Furthermore, the average results of the real densities of the Portland cements were higher due to higher clinker content. Average density values for concretes used in thermal storage are around 2200 kg·m^{-3} [26] and, considering the cement density has a direct influence on the density of the concrete produced, the values obtained for LC^3 cements were optimal for this application. In addition, as with apparent density, a high real density indicates a higher heat storage capacity. This is essential for TES systems, as it allows significant amounts of thermal energy to be retained and released when required. However, after 500 h at 350 °C, the cements showed noticeable changes in weight and size, as well as small fractures on some of their faces. Because of this, the apparent densities of the materials were reduced by 16.42 % for MK, 20.98 % for AM, 15.79 % for Portland D, and 17.14 % for Portland SR. The difference between MK and MA could be because unreacted MK has no hydroxyls and unreacted MA does. This reduction is important since it reaches values of 15–20 %. This can have a strong impact on its application as a thermal storage system, causing the capacity to store heat to be significantly reduced.

As for the porosity obtained for Portland and LC^3 cements, both MA and Portland SR were 16 %. In addition, the use of MK and MA reduced the pore volume present in the sample by 24 % and 40 % concerning CEM II (Portland D). This large number of pores in Portland D is also related to its low compressive strength since it is easier for fractures to occur in the areas close to the voids. In addition, the presence of MK implied a higher number of pores compared to MA. Studies indicate that the total porosity increases when metakaolin is used as a partial substitute for clinker [29,30]. However, this increase in porosity does not

Table 2
Summary of the properties of each type of cement before and after thermal aging.

Cement type		Before aging							After aging			
		Physicochemical and mechanical properties				Thermal properties (RT)			Physicochemical and mechanical properties		Thermal properties (RT)	
		σ_c (MPa)	ρ_{bulk} (kg/m^3)	ρ_{real} (kg/m^3)	ϕ (%)	C_p (J·g^{-1}·°C^{-1})	ρ_e (MJ·m^{-3}·°C^{-1})	k (W·m^{-1}·K^{-1})	σ_c (MPa)	ρ_a (kg/m^3)	C_p (J·g^{-1}·°C^{-1})	ρ_e (MJ·m^{-3}·°C^{-1})
LC^3	MK	45.03	1770.14	2217.88	20.18	0.72	1.18	0.75	25.71	1422.62	0.75	1.07
	MA	43.19	1768.70	2099.71	15.76	0.76	1.34	0.74	24.71	1386.65	0.58	0.80
PC	D	40.00[a]	1786.10	2434.51	26.63	0.77	1.38	1.04	10.22	1503.99	0.91	1.37
	SR	52.00[a]	1958.63	2344.99	16.48	0.84	1.64	1.13	18.30	1622.84	0.99	1.61

[a] Values obtained from the manufacturer's technical datasheet [25].

depend so much on the MK content, it is more related to its presence or not in the mixture [30]. Likewise, solid aggregates represent approximately three-quarters of the total volume of concrete, so their own porosity has an impact on the total porosity of the concrete [31]. Therefore, having adequate porosity values in the samples will be reflected in the properties of the concrete made from these cements. In summary, a lower porosity allows a better heat transfer inside the material with a more homogeneous and efficient heat distribution.

From the XRD performed for each of the samples, the corresponding phases for each type of cement were obtained (Fig. 2). On the one hand, calcite was the major component for the four cements under study, because it is a calcium carbonate, derived from limestone for the formation of clinker. In addition to this mineral, there was a strong presence of calcium hydroxide, especially in the PCs. This is because the silica and alumina in the clay consumed part of the Ca(OH)$_2$ with pozzolanic reactions, making its presence lower in cements with kaolin as a partial substitute for clinker. Likewise, the diffractograms showed an amorphous phase, which is due to the C-(A)-S-H that is the main reaction product, and which acts as a binder. In LC^3, the presence of unreacted amorphous clay could also contribute to the intensity of the amorphous halo. They also showed phases from the unreacted tricalcium silicate (C$_3$S) and tetracalcium aluminoferrite (C$_4$AF) of the clinker. Both portlandite and ettringite are phases resulting from the hydration of Portland cement clinker. The ettringite peaks in the four samples were attributed to reactions between sulphates and calcium aluminates. The presence of this phase in cement has been shown to

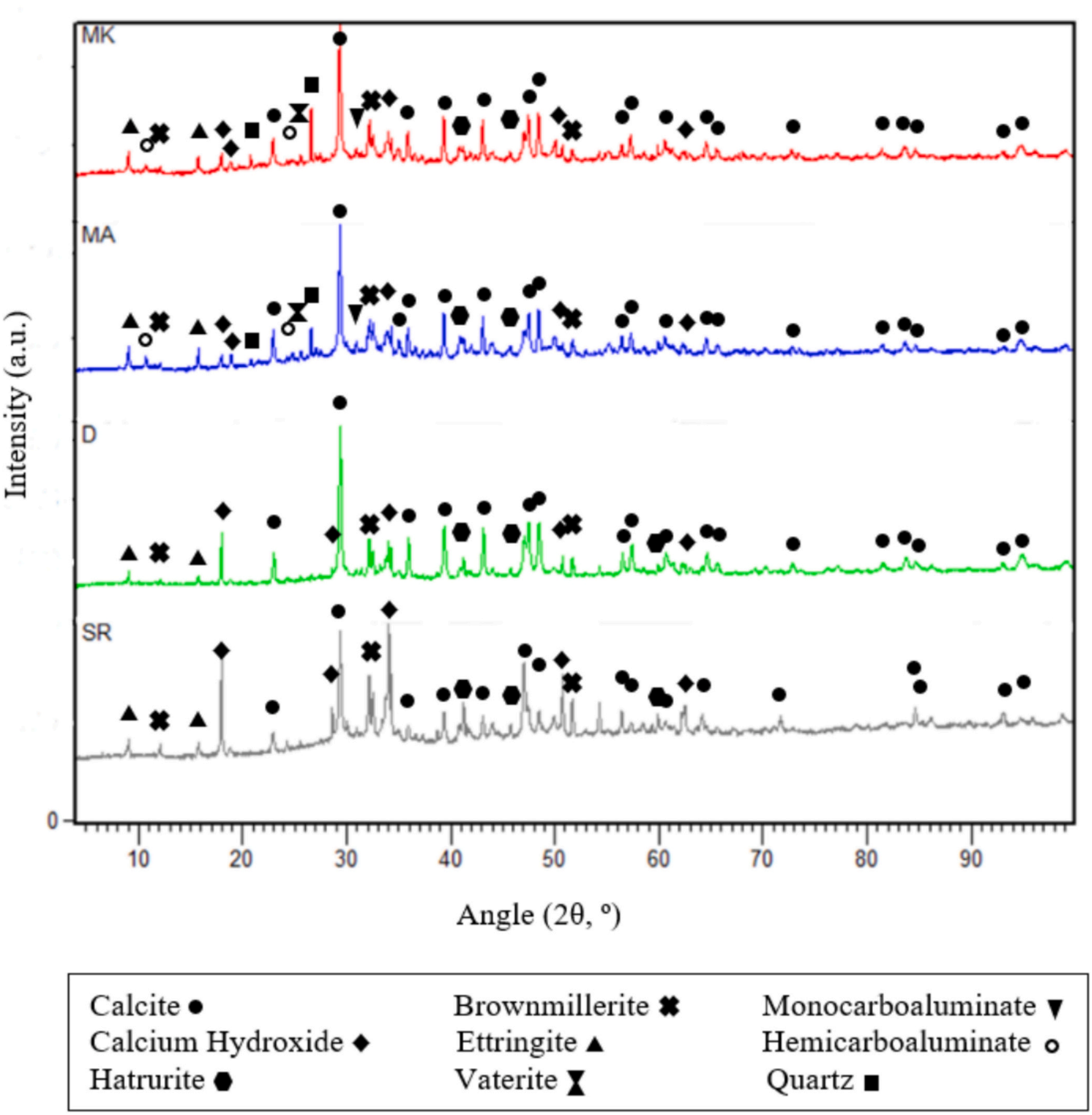

Fig. 2. X-ray diffractograms of cements.

contribute significantly to both strength and durability [32], which helps explain the high compressive strength values observed in LC^3. It is also worth noting the occurrence of vaterite in LC^3s, along with quartz, likely originating from clay impurities. On the other hand, the main difference between LC^3s and PCs was the presence of carboaluminate phases, specifically monocarboaluminate and hemicarboaluminate. These compounds also play a crucial role in mechanical strength, thus contributing to the preservation of adequate performance despite the 50 % substitution of clinker.

3.2. Thermal properties

Table 2 shows the C_p and ρ_e for each type of cement. The heat capacities obtained for LC^3s were like those of Portland D, which has 30 % limestone. However, if compared with the results of Portland SR, which has 94 % clinker, the partial substitution of clinker, using 30 % kaolin and 15 % of limestone, did affect this thermal property of the material. Likewise, according to the bibliography [33,34], clinker has a heat capacity of 0.87–0.90 $J \cdot g^{-1} \cdot {}^\circ C^{-1}$ for temperatures between 300 and 400 °C. This explains the C_p result obtained for Portland SR, since it has an extremely high content of this material. In addition, according to the literature [6,7], to use concrete as a thermal storage system, it must have C_p values from 0.7 to 1.0 $J \cdot g^{-1} \cdot {}^\circ C^{-1}$ in a temperature range from 25 °C to 400 °C. However, there are studies [26] indicating that due to the reactions that take place when concrete is heated, the specific heat decreases in the temperature range between 20 °C and 120 °C. Therefore, the values obtained were not influenced by this decrease, since they are not in the indicated temperature range. In thermal storage, the heat capacity of concrete depends mainly on the aggregates used in the mix, gravel, and sand. These have a higher heat capacity, so the effect of cement on the performance of thermal storage concrete is not as critical. In terms of heat storage capacity per unit volume, Portland SR showed the highest values because its density and C_p were higher than the rest of the cements. For the rest of the samples, although the three materials presented similar densities, the differences in heat capacity caused the MK to obtain slightly lower values than the rest. As with the pre-aging values, the results obtained after heat treatment showed a clear difference between OPCs and LC^3s. It was observed that the C_p increased for all samples except mechanically activated kaolin. However, due to the density variation after thermal aging, the volumetric heat capacity values were not affected, except for MA. This large change may have been caused by the large amount of mass lost by the material. Because of this, it can be stated that temperature aging did not affect the ability of the cements to absorb heat, excluding MA.

Finally, thermal conductivity results showed that the cements with higher clinker content have a higher k. Portland SR, whose clinker content is 94 %, showed an average value of 1.13 $W \cdot m^{-1} \cdot K^{-1}$; Portland D, whose content is 70 %, had a conductivity of 1.04 $W \cdot m^{-1} \cdot K^{-1}$; and LC^3, with a proportion of 50 %, achieved the lowest results around 0.74–0.75 $W \cdot m^{-1} \cdot K^{-1}$. For use as TES, the materials must have a high conductivity to facilitate heat transfer to the fluid circulating in the inner tubes. The results showed that LC^3s have a lower conductivity than PCs. This would imply that their use in thermal storage could affect the amount of heat stored. However, normal values for cement are in the range of 0.20–0.80 $W \cdot m^{-1} \cdot K^{-1}$ [35], so the results obtained were favourable. In addition, for a better interpretation of the results, it would be more appropriate to calculate the thermal conductivity of the cement samples at the temperature of use as TES, since this variable decreases with increasing temperature. There is evidence that in a range from 20 °C to 280 °C, this decreases because of internal transformations of the concrete due to heating [26].

4. Life cycle assessment (LCA)

LCA is a systematic analytical tool designed to assess the environmental impact of products or processes following ISO 14040 Standards [36]. It can be performed from the entire life cycle (cradle-to-grave perimeter) or one to several stages of the life cycle. This tool makes it possible to identify and quantify the resources and raw materials consumed, as well as emissions to water, air, and soil [37]. The typical steps of an LCA are 1) Goal and scope definition, which involves setting functional units, system boundaries, and analysis limits. This step allows for identifying the beginning and end points in the life cycle of a product or process and for specifying the processes that will be assessed, 2) The life cycle inventory analysis (LCI) that encompasses collecting data and performing calculations to measure the inputs and outputs of materials and energy connected to the product system under investigation, 3) The life cycle impact assessment (LCIA) which entails the association of inventory data with impacts and the valuation of these impacts, allowing the evaluation of the effects on the environment and human health, and finally 4) The life cycle interpretation, which evaluates the results to draw conclusions and to make decisions [37,38].

4.1. Goal and scope

This LCA aims to determine the environmental feasibility of substituting traditional OPC cement with LC^3 in the production of the concrete used as a TES material for implementation in CSP plants. The environmental impacts of the understudied concretes are compared based on the different compositions of the manufactured cements: a) The new LC^3 option using 30 % thermally activated kaolin and 15 % limestone as SCMs, and b) The ordinary Portland Cement (OPC) that uses 95 % clinker. The functional unit chosen was 1 t of concrete produced. The system boundaries range from the extraction of raw materials to the final manufacturing of concrete (cradle-to-gate perimeter). Key processes taken into consideration encompass clinkerization, clay calcination, grinding, and mixing (Fig. 3).

4.1.1. Life cycle inventory analysis

Table 3 shows the inventory of materials and energy to produce 1 t of concrete. This inventory was sized and organized considering the following aspects:

- Raw material for clinkerization was categorized into the following four main components: limestone 88 %, clay (alumina) 9 %, silica 2 %, and iron ore 1 %. On average, 1.58 tons of raw materials are needed to produce either 0.95 tons of clinker or 1.0 ton of finished traditional OPC cement [40]. These materials are crushed, mixed, and calcined in a kiln at 1450 °C, which leads to a significant generation of CO_2 emissions, cement kiln dust, and particulate matter [41].
- Based on experimental and production data, the material proportions used for manufacturing the cements were as follows: OPC (95 % clinker and 5 % gypsum) and LC^3 (50 % clinker, 30 % calcined kaolinitic clay, 15 % limestone, and 5 % gypsum) [42].
- The mass proportion of cement, sand, gravel, and water used for the concrete mix was 1:1.52:3.21:0.49, as this ratio is recognized for offering the optimal strength-to-cost balance for use in TES applications [43].
- It was assumed that all processes take place within the same facility. The data inventory was structured bearing in mind an industrial technology level, enabling the conversion of a wet cement kiln into a clay calciner.
- Regarding energy input data, it is known that cement kiln operations primarily rely on coal, petroleum coke, and various fuels or waste materials. The exact blend of fuel sources varies significantly depending on the manufacturing facility and may encompass natural gas, fuel oil, tires, and others [40]. For this study, three primary fuel sources were chosen: Pet coke for clinkerization, fuel oil for cement production, and gas oil for concrete mixing.
- In the production of LC^3, the energy consumed for clay calcination was estimated at 2.6 MJ/kg, derived from theoretical calculations

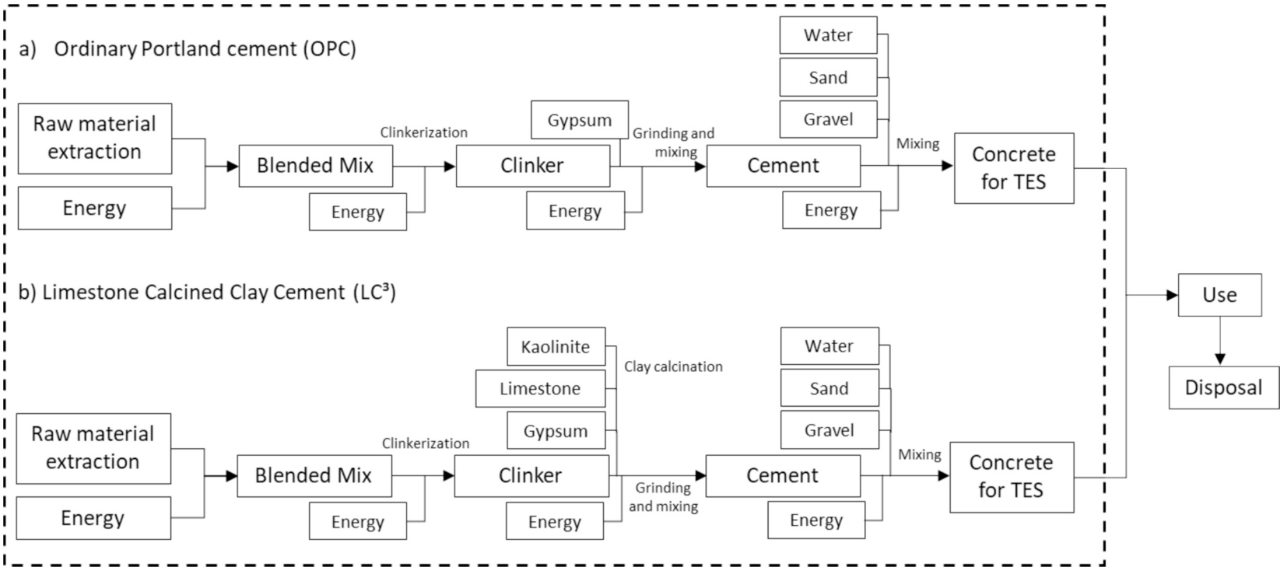

Fig. 3. System's boundaries: a) Concrete made of ordinary Portland cement (OPC) and b) Concrete made of Limestone Calcined Clay Cement (LC^3). Adapted from: [39].

Table 3
Inventory of materials required to produce 1 t of concrete for TES applications.

Process	Inventory	LC^3	OPC
Clinker production	Materials (kg)		
	Limestone	70.8	134.5
	Clay	7.2	13.8
	Sand	1.6	3.1
	Iron ore	0.8	1.5
	Energy for clinkerization (MJ)		
	Electricity	25.4	46.3
	Pet coke	309.5	568.3
Cement production	Materials (kg)		
	Kaolinite	48.2	0
	Limestone	24.1	0
	Gypsum	8.0	8.0
	Clinker	80.4	152.8
	Energy for clay calcination (MJ)		
	Electricity	6.6	0
	Fuel oil	118.8	0
	Energy for cement production (MJ)		
	Electricity	13.8	30.1
Concrete production	Materials (kg)		
	Water	78.8	78.8
	Sand	244.4	244.4
	Gravel	516.1	516.1
	Cement	160.8	160.8
	Energy for concrete mixing (MJ)		
	Electricity	33.7	33.3
	Gas oil	33.7	33.3

conducted by [42]. The energy required for cement grinding and mixing is 187 MJ/t for OPC cement and 86 MJ/t for LC^3 cement [39]. Additionally, the energy demand for concrete mixing amounts to 0.1060 Gj/m^3, covering tasks such as aggregate and cement stacking at the production plant, blending of aggregate, cement, and water at the batching plant, and loading the concrete onto the truck [44].

- Finally, it was assumed that the electricity usage relies on the European electricity mix.

The inventory data was modelled using the Ecoinvent database [45], and the Software GaBi [46] was employed to evaluate the comprehensive environmental impacts. The analysis was conducted using the following methods: a) IPCC 2013, which characterizes gaseous emissions according to their global warming potential (GWP) [47], and b) ReCiPe, which quantifies the environmental alterations in impact points [48].

4.1.2. *Impact assessment (LCIA)*

The results of the IPCC GWP 2013 (Table 4) indicate that 37.3 kg of CO_2 equivalent is produced per ton of LC^3 concrete. In the case of OPC, the emissions reach 48.9 kg of CO_2 equivalent per ton. This confirms that replacing a part of the clinker mineral with kaolinite clay constitutes a manner of reducing GWP emissions. In the studied case, the emissions reduction achieved by the competitive LC^3 solution amounts to 23.8 %.

On the other hand, the global environmental impact calculated through the ReCiPe indicator is shown in Fig. 4. The ternary mix receives 22.6 % fewer impact respect to OPC (Fig. 3-**a**). For both cases, clinker production has a major relative contribution to the impact account (Fig. 3-**b**).

4.1.3. *Interpretation*

The material inventory shows the ternary mix concrete (LC^3) contains an embodied energy of 542 MJ/t. Whereas, for the typically implemented option (OPC) 711 MJ/t is required. By using kaolinitic clay in LC^3, energy savings of 160 MJ/t are possible to achieve. The lower energy intensity associated with the LC^3 improves the energy efficiency associated with TES systems in CSP plants.

Regarding the global warming potential, the results show how alternative cement mixes can effectively diminish the overall global CO_2 emissions of concrete production for TES applications. The IPCC 2013 indicator has also evidenced that fossil fuels are the main contributor to the GWP in the concrete life cycle, causing more than 50 % of the total GWP of both concrete types (LC^3 and OPC), mostly due to the clinkerization that commonly uses pet coke as the main energetic source.

Likewise, the ReCiPe impact indicator shows that most of the LC^3 impact reduction is achieved during the clinkerization process. The impact of the cement production stage is higher in the ternary mix, primarily due to the energy required for the thermal activation of kaolin (clay calcination) and the incorporation of new raw materials. Nevertheless, the total impact point count continues to be higher in the traditional product (OPC) because it uses more clinker, the main contributor to the impact account [40,42]. As expected, the concrete production stage has a similar impact contribution in both cases.

Table 4
Global warming potential and flows relative contribution to CO_2 equivalent emissions.

IPCC GWP 2013 (kg CO_2 Equiv. / t)		Variation (%)	LC^3 relative contribution (%)			OPC relative contribution (%)		
LC^3	OPC		Energy: fuels	Energy: electricity	Raw materials	Energy: fuels	Energy: electricity	Raw materials
37.3	48.9	23.8	57	31	12	57	33	10

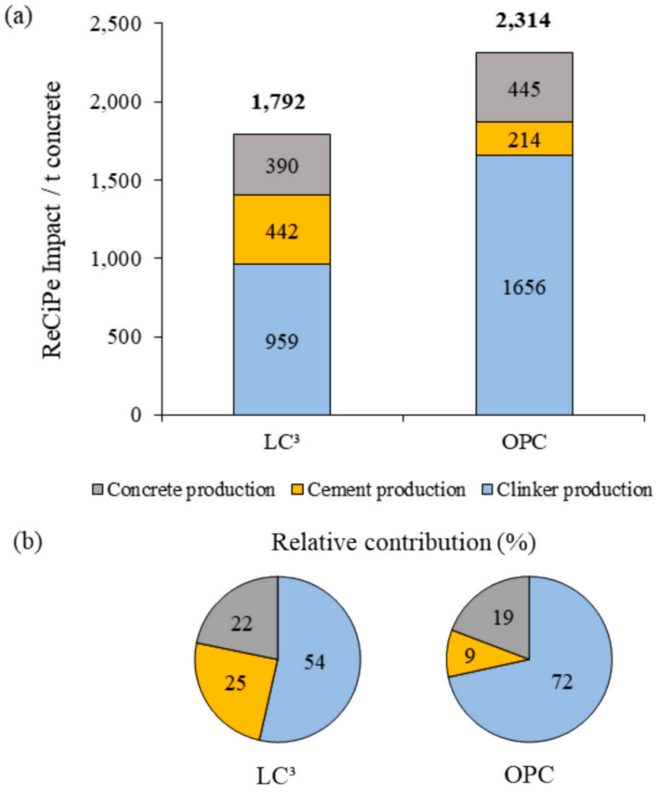

Fig. 4. ReCiPe environmental impact, (a) Comparison of total impact per ton of concrete produced (LC^3 vs OPC). (b) The relative contribution of production processes for both concretes.

5. Conclusions

The compressive strength of LC^3 shows that the mechanical behavior of this cement under working mechanical requirements will be similar to those performed by the common cements reported in the literature. Likewise, the densities of this type of cement are like those of CEM II cements and close to those of CEM I cements and their contribution to the energy density will be similar as well. This implies that the mechanical and thermal amorphization of the kaolin (using 30 % of it in the mix) was sufficient to reach adequate values.

Similarly, the thermal properties under study demonstrated the proper capacity of this type of cement to store thermal energy. The heat capacity values, both per unit mass and per unit volume, are at the level of PCs. On the other hand, the thermal conductivities are slightly lower but still meet the system's requirements. In addition to this, the variations observed in the behavior of LC^3 after thermal aging allow for evaluating how they would affect the conditions of use as TES. Therefore, the LC^3 cement is a proper candidate to store thermal energy in blocks. This study confirms that partially replacing clinker with LC^3 enables the development of more sustainable concrete materials for TES applications in CSP systems. The LCA demonstrates that the LC^3-based concrete significantly reduces both energy consumption and greenhouse gas emissions compared to conventional OPC-based concrete. Key findings reveal a 23.8 % reduction in CO_2-equivalent emissions (37.3 kg/t for LC^3 vs. 48.9 kg/t for OPC) and 22.6 % lower overall environmental impact (ReCiPe indicator) through the ternary blend formulation. This emission reduction stems primarily from two synergistic mechanisms:

- Reduced clinker content (50 % vs. 95 % in OPC), mitigating energy-intensive calcination.
- Optimal utilization of SCMs (30 % calcined kaolin +15 % limestone)

Although the calcination of clay introduces additional energy demands, its overall environmental footprint remains lower than that of OPC, making LC^3 a more sustainable option. Within the defined boundaries and assumptions, LC^3 emerges as a viable and environmentally beneficial alternative to OPC for the manufacture of TES concrete in CSP infrastructure. Its adoption can meaningfully enhance the sustainability of TES systems during the manufacturing phase of CSP plants.

CRediT authorship contribution statement

L. Betancor-Cazorla: Writing – original draft, Investigation, Data curation, Methodology, Formal analysis, Conceptualization. **Carlos A. Vielma:** Data curation, Software, Writing – original draft, Investigation, Conceptualization. **J. Mañosa:** Methodology, Supervision, Investigation, Conceptualization, Data curation. **S. Dosta:** Conceptualization, Visualization, Resources, Writing – review & editing, Investigation, Supervision, Project administration. **J.M. Chimenos:** Writing – review & editing, Investigation, Project administration, Data curation, Resources. **C. Barreneche:** Supervision, Investigation, Formal analysis, Methodology, Funding acquisition, Data curation, Writing – review & editing, Conceptualization.

Declaration of competing interest

The authors declare that they have no known competing financial interests or personal relationships that could have appeared to influence the work reported in this paper.

Acknowledgments

The authors would like to thank the Catalan Government for the quality accreditation given to their research group DIOPMA (2021 SGR 00708 & 2021 SGR 00512). DIOPMA is a certified agent TECNIO in the category of technology developers from the Government of Catalonia. The authors are grateful to the companies Minerals i Derivats, S.A. and COM-CAL for the supply of the raw clay, to Cementos Molins S.A. for providing the clinker and to CHRYSO Spain for supplying the superplasticizer. This work has been partially funded by the Spanish government PID2021-123511OB-C32 (MICINN/FEDER, UE) and supported by "100 Foreign Experts Plan of Hebei Province". This work couldn't be carried out without the support of "Thermodust" project (n. 101046835) funded by the "Horizon Europe" framework programme, and CDTI and NextGeneration EU funds for the Bioenergy project MIP-20221004.

Data availability

Data will be made available on request.

References

[1] International Energy Agency (IEA), "World energy outlook." Accessed: Sep. 03, 2024. [Online]. Available: https://www.iea.org/reports/world-energy-outlook-2022.

[2] United Nations Framework Convention on Climate Change (UNFCCC), "The Paris agreement," 2016, *UN*. Accessed: Sep. 03, 2024. [Online]. Available: https://unfccc.int/sites/default/files/resource/parisagreement_publication.pdf.

[3] Oficina de Publicaciones de la Unión Europea. "Pacto Verde Europeo: consecución de nuestros objetivos," 2021, Publications Office of the European Union, Luxemburgo. [Online]. Available: https://doi.org/10.2775/948427.

[4] H.L. Zhang, J. Baeyens, J. Degrève, G. Cacères, Concentrated solar power plants: Review and design methodology, Renew. Sustain. Energy Rev. 22 (2013) 466–481, https://doi.org/10.1016/j.rser.2013.01.032.

[5] A. Palacios, C. Barreneche, M.E. Navarro, Y. Ding, Thermal energy storage technologies for concentrated solar power – A review from a materials perspective, Renew. Energy 156 (2020) 1244–1265, https://doi.org/10.1016/j.renene.2019.10.127.

[6] N. Hoivik, et al., Long-term performance results of concrete-based modular thermal energy storage system, J Energy Storage 24 (2019) 100735, https://doi.org/10.1016/j.est.2019.04.009.

[7] D. Laing, W.-D. Steinmann, R. Tamme, C. Richter, Solid media thermal storage for parabolic trough power plants, Sol. Energy 80 (10) (2006) 1283–1289, https://doi.org/10.1016/j.solener.2006.06.003.

[8] D. Laing, D. Lehmann, C. Bahl, *Concrete storage for solar thermal power plants and industrial process heat*, vol, in: IRES III 2008, 2008. Stuttgart. Accessed: Sep. 03, 2024. [Online]. Available: https://elib.dlr.de/57976/1/2008_IRES_III_Concrete_Storage_Laing_et_al.pdf.

[9] ECRETE, Energy storage solutions based on concrete, Accessed: Apr. 15 (2025) [Online]. Available: https://ecrete.org/.

[10] M. Rahjoo, G. Goracci, J.J. Gaitero, P. Martauz, E. Rojas, J.S. Dolado, Thermal energy storage (TES) prototype based on geopolymer concrete for high-temperature applications, Materials 15 (20) (2022) 7086, https://doi.org/10.3390/ma15207086.

[11] M. Rahjoo, G. Goracci, P. Martauz, E. Rojas, J.S. Dolado, Geopolymer concrete performance study for high-temperature thermal energy storage (TES) applications, Sustainability 14 (3) (2022) 1937, https://doi.org/10.3390/su14031937.

[12] M. Rahjoo, E. Rojas, G. Goracci, J.J. Gaitero, P. Martauz, J.S. Dolado, A numerical study of geopolymer concrete thermal energy storage: Benchmarking TES module design and optimizing thermal performance, J Energy Storage 74 (2023) 109389, https://doi.org/10.1016/j.est.2023.109389.

[13] A. Palacios, C. Barreneche, M.E. Navarro, Y. Ding, Thermal energy storage technologies for concentrated solar power – A review from a materials perspective, Renew. Energy 156 (2020) 1244–1265, https://doi.org/10.1016/j.renene.2019.10.127.

[14] CADE Engineered Technologies, "solidTES – Almacenamiento Térmico," Mar. 09, 2018, *2024*. [Online]. Available: https://cadeengineering.com/es/solidtes/page/2/.

[15] CBS News, "Cement industry accounts for about 8% of CO2 emissions," Jan. 16, 2023. Accessed: Sep. 03, 2024. [Online]. Available: https://www.cbsnews.com/news/cement-industry-co2-emissions-climate-change-brimstone/.

[16] Global Cement and Concrete Association, "Concrete future," Oct. 12, 2021, *London*. Accessed: Sep. 03, 2024. [Online]. Available: https://gccassociation.org/concretefuture/wp-content/uploads/2021/10/GCCA-Concrete-Future-Roadmap-Document-AW.pdf.

[17] World Resources Institute and World Business Council for Sustainable Development, "The Greenhouse Gas Protocol," May 2004, USA. Accessed: Sep. 03, 2024. [Online]. Available: https://gccassociation.org/concretefuture/wp-content/uploads/2021/10/GCCA-Concrete-Future-Roadmap-Document-AW.pdf.

[18] A.M. Rashad, Metakaolin as cementitious material: History, scours, production and composition – A comprehensive overview, Constr. Build. Mater. 41 (2013) 303–318, https://doi.org/10.1016/j.conbuildmat.2012.12.001.

[19] Scrivener, K., Martirena, F., Bishnoi, S., and Maity, S. Calcined Clay Limestone Cements (LC3). Dec. 01, 2017. Elsevier Ltd. https://doi.org/10.1016/j.cemconres.2017.08.017.

[20] E. Badogiannis, G. Kakali, S. Tsivilis, Metakaolin as supplementary cementitious material: Optimization of kaolin to metakaolin conversion, J. Therm. Anal. Calorim. 81 (2005), https://doi.org/10.1007/s10973-005-0806-3.

[21] R. Fernandez, F. Martirena, K.L. Scrivener, The origin of the pozzolanic activity of calcined clay minerals: A comparison between kaolinite, illite and montmorillonite, Cem. Concr. Res. 41 (1) (2011) 113–122, https://doi.org/10.1016/j.cemconres.2010.09.013.

[22] B. Ilić, V. Radonjanin, M. Malešev, M. Zdujić, A. Mitrović, Study on the addition effect of metakaolin and mechanically activated kaolin on cement strength and microstructure under different curing conditions, Construct. Build Mater. 133 (2017) 243–252, https://doi.org/10.1016/j.conbuildmat.2016.12.068.

[23] A. Svobodova-Sedlackova, et al., Using statistical analysis to create a new database of Nanofluids' specific heat capacity, J. Mol. Liq. 369 (2023) 120847, https://doi.org/10.1016/j.molliq.2022.120847.

[24] B. Ilić, V. Radonjanin, M. Malešev, M. Zdujić, A. Mitrović, Effects of mechanical and thermal activation on pozzolanic activity of kaolin containing mica, Appl. Clay Sci. 123 (2016) 173–181, https://doi.org/10.1016/j.clay.2016.01.029.

[25] Molins Cement, "Cementos Molins Industrial," 2024, *Barcelona*. [Online]. Available: https://www.cmi.cemolins.es/.

[26] A. Gil, et al., State of the art on high temperature thermal energy storage for power generation. Part 1-concepts, materials and modellization, Renewable and Sustainable Energy Reviews (2010), https://doi.org/10.1016/j.rser.2009.07.035.

[27] F. Avet, E. Boehm-Courjault, K. Scrivener, Investigation of C-A-S-H composition, morphology and density in limestone calcined clay Cement (LC3), Cem. Concr. Res. 115 (2019) 70–79, https://doi.org/10.1016/j.cemconres.2018.10.011.

[28] Código Técnico de la Edificación (CTE), "Documento Básico de Seguridad Estructural-Acciones en la Edificación (SE-AE)," Apr. 2009. Accessed: Sep. 03, 2024. [Online]. Available: https://www.codigotecnico.org/pdf/Documentos/SE/DBSE-AE.pdf.

[29] F. Zunino, K. Scrivener, The reaction between metakaolin and limestone and its effect in porosity refinement and mechanical properties, Cem. Concr. Res. 140 (2021) 106307, https://doi.org/10.1016/j.cemconres.2020.106307.

[30] M. Frías, M. de Sanches Rojas, Influence of the metakaolin on porous structure of matrixes based in mk/cement, Materiales De Construccion - MATER CONSTR 50 (2000) 57–67, https://doi.org/10.3989/mc.2000.v50.i259.399.

[31] R. Solís, M. Alcocer, Durabilidad del concreto con agregados de alta absorción, Ing. Investig. Tecnol. 20 (4) (2019) 1–13, https://doi.org/10.22201/fi.25940732e.2019.20n4.039.

[32] J. Liu, W. Zhang, Z. Li, H. Jin, W. Liu, L. Tang, Investigation of using limestone calcined clay cement (LC3) in engineered cementitious composites: The effect of propylene fibers and the curing system, J. Mater. Res. Technol. 15 (2021) 2117–2144, https://doi.org/10.1016/j.jmrt.2021.09.023.

[33] O. Labahn and B. Kohlhaas, Prontuario del Cemento, 5th ed. Barcelona, 1985. Accessed: Sep. 03, 2024. [Online]. Available: https://books.google.es/books?hl=es&lr=&id=9UO8F9deIuwC&oi=fnd&pg=IA5&dq=B.+K.+Otto+Labahn,+Prontuario+del+Cemento,+5th+ed.+Barcelona,+1985&ots=PeCZ8axBU7&sig=gT-IqRiZGWOQWQJtTaCmJLM2Tf8#v=onepage&q&f=false.

[34] J. Rincón, Evaluación del consumo calórico en la producción de clinker en un horno rotatorio vía seca a partir de un análisis basado en balances de masa y energía, Accessed (2024) [Online]. Available: https://www.virtualpro.co/files-bv/20120201/20120201-015.pdf.

[35] R. Maddalena, J.J. Roberts, A. Hamilton, Can Portland cement be replaced by low-carbon alternative materials? A study on the thermal properties and carbon emissions of innovative cements, J. Clean. Prod. 186 (2018) 933–942, https://doi.org/10.1016/j.jclepro.2018.02.138.

[36] International Organization for Standardization, *Environmental management—Life cycle assessment—Principles and framework (Vol. 14040). (2006)*. 2006.

[37] K.-M. Lee, A. Inaba, Life cycle assessment best practices of ISO 14040 series Ministry of Commerce, industry and energy Republic of Korea Asia-Pacific economic cooperation committee on trade and investment, Korea (2004).

[38] Klöpffer, Walter and Grahl, Birgit. Life Cycle Assessment (LCA) a Guide to Best Practice. Weinheim, Germany. 2014.

[39] S. Sánchez Berriel, et al., Assessing the environmental and economic potential of limestone calcined clay Cement in Cuba, J. Clean. Prod. 124 (2016) 361–369, https://doi.org/10.1016/j.jclepro.2016.02.125.

[40] D.N. Huntzinger, T.D. Eatmon, A life-cycle assessment of Portland cement manufacturing: Comparing the traditional process with alternative technologies, J. Clean. Prod. 17 (7) (2009) 668–675, https://doi.org/10.1016/j.jclepro.2008.04.007.

[41] J. Sjunnesson, "Life Cycle Assessment of Concrete," 2005. [Online]. Available: www.miljo.lth.se.

[42] Gettu, R. and Basavaraj, A. "Life Cycle Assessment of LC3: Parameters and Prognoses," 2020. [Online]. Available: http://www.springer.com/series/8781.

[43] C.R.C. Rao, H. Niyas, P. Muthukumar, Performance tests on lab–scale sensible heat storage prototypes, Appl. Therm. Eng. 129 (2018) 953–967, https://doi.org/10.1016/j.applthermaleng.2017.10.085.

[44] G. Heravi, T. Nafisi, R. Mousavi, Evaluation of energy consumption during production and construction of concrete and steel frames of residential buildings, Energ. Buildings 130 (2016) 244–252, https://doi.org/10.1016/j.enbuild.2016.08.067.

[45] G. Wernet, B. C., B. Steubing, J. Reinhard, E. Moreno-Ruiz, and B. Weidema, "Ecoinvent Version 3," 2016, Ecoinvent, Zurich, Switzerland: 3.9.1.

[46] Sphera, "Product sustainability GaBi database," 2017, Sphera, Stuttgart, Germany.: LCA for Experts.

[47] R. Hischier, et al., Implementation of Life Cycle Impact Assessment Methods. Ecoinvent Report No. 3, v2.2, Dübendorf, 2010.

[48] S. Huijbregts, Z. Steinmann, P. Elshout, G. Stam, ReCiPe 2016 v1.1 a harmonized life cycle impact assessment method at midpoint and endpoint level report I: Characterization, The Netherlands (2017) [Online]. Available: www.rivm.nl/en.